Original articles

Applying chemical shift images (in-phase/opposed phased) for differentiating low-grade from high-grade glioma and comparison with magnetic resonance spectroscopy

Bita Abbasi[1] · Afshar Ghamari Khameneh[1] · Hadi Zareh Soltaniye[1] · Gisoo Darban Hosseini Amirkhiz[2] · Ehsan Karimi[1] · Reza Akhavan[3]

[1] Department of Radiology, Faculty of Medicine, Imam Reza Hospital, Mashhad University of Medical Sciences, Mashhad, Iran; [2] Research Center for Prevention of Cardiovascular Disease, Institute of Endocrinology and Metabolism, Iran University of Medical Sciences (IUMS), Tehran, Iran; [3] Department of Emergency Medicine, Faculty of Medicine, Mashhad University of Medical Sciences, Mashhad, Iran

Abstract

Background: Grading gliomas is essential for treatment decisions and patient prognosis. In this study we evaluated the in-phase and out-of-phase sequences for distinguishing high-grade (HGG) from low-grade glioma (LGG) and the correlation with magnetic resonance spectroscopy (MRS) results.
Methods: This observational study comprised patients with brain tumors referred to our center for brain MRS. The gold standard for diagnosis was based on the World Health Organization (WHO) glioma classification. A standard tumor protocol was accomplished using a 1.5-T MRS scanner. Before contrast medium administration, extra in- and out-phase sequences were acquired. Three $20-30\text{-mm}^2$ oval regions of interest (ROIs) were placed in the solid component and the signal loss ratio (SLR) was calculated with the following formula:
$$SLR_{tumor} = (SI_{In\ phase} - SI_{Opposed\ phase}) / SI_{In\ phase}$$
Correlations and comparisons between groups were made using the Pearson, chi-square and, independent samples t tests. Receiver operating characteristic (ROC) curve analysis was performed to assess the diagnostic performance. Statistical significance was set at $p < 0.05$.
Results: In total, 20 patients were included in the LGG and 13 were included in the HGG group. The mean SLR in the HGG and LGG groups was 3.66 ± 2.12 and 1.63 ± 1.86, respectively ($p = 0.01$). There was a statistically significant correlation between lipid lactate (0.48, $p = 0.004$) and free lipid (0.44, $p = 0.009$) concentrations on MRS with SLR.
Conclusions: The SLR is a simple, rapid, and noninvasive marker for differentiating between LGG and HGG. There is a significant correlation with both the concentration and presence of free lipid and lipid-lactate peaks in MRS.

Keywords
MRI · Cerebral · Magnetic resonance spectroscopy · Glioma · Brain tumor

Target
- 54 patients with brain masses who were referred to our imaging center for MRS underwent chemical shift GE IOP sequence(2020-2022)

Excluded
- 11 non-glioma tumors (metastais and lymphoma)
- 10 poor quality image examination

Included
- 33 patients with 33 gliomas
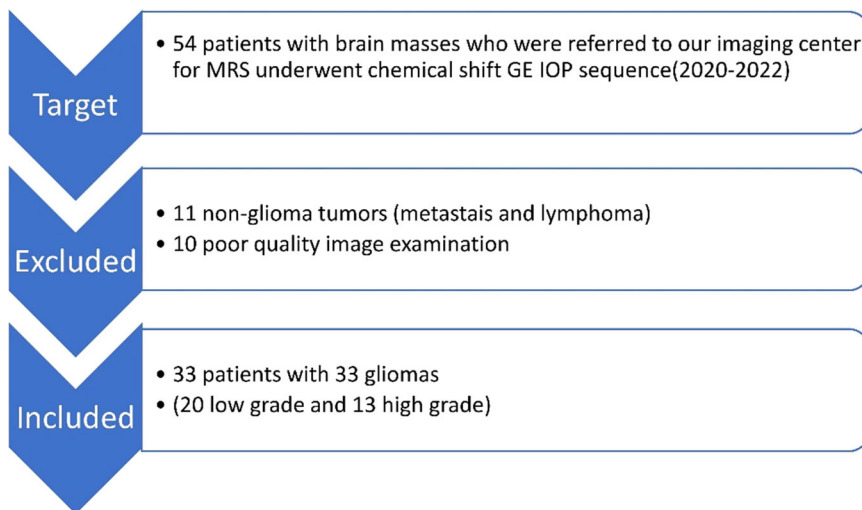- (20 low grade and 13 high grade)

Fig. 1 ▲ Flowchart of the selection process. *GE* gradient-echo sequence, *IOP* in-phase and opposed-phase sequence

Background

The most common primary brain malignancies are gliomas (approximately 80%) [1]. The incidence and 5-year survival rate are 1–4 per 100,000 and 4–40%, respectively. The grade of the central nervous system tumors, classified by the World Health Organization (WHO), determines the survival rate and management plan. According to this classification, gliomas are divided into four grades. Grades 1 and 2 are considered low-grade glioma (LGG) and grades 3 and 4 are considered high-grade glioma (HGG; [2, 3]). If LGGs are resected at the time of diagnosis, the 5-year survival rate is 94% and 51.6% for grades 1 and 2, respectively [4–6]. The treatment and prognosis for high-grade gliomas vary greatly. They usually require radiation therapy and chemotherapy after surgery, and the 5-year survival rate is only 25.2% and 8.9% for grades 3 and 4, respectively. [5–7].

Although histological tests are the gold standard for the diagnosis of glioma, they have certain limitations such as high invasiveness, bleeding and infection, and likelihood of sampling errors, and they are prone to inter- and intra-neuropathologist variability. Complications can arise depending on the location and grade of the tumors [8]. Imaging has the advantage that histopathological tumor changes can be visualized indirectly and non-invasively. Magnetic resonance imaging (MRI)

is the imaging method of choice for the detailed characterization of brain tumors, since it provides valuable information on tumor composition, anatomical location, edema, hemorrhage, adjacent brain tissue, and mass effect [9]. Additionally, contrast enhancement indicates neovascularization or disruption of the blood–brain barrier, which is an important feature of HGG. Despite these advantages, conventional MRI has a limited role in grading gliomas due to its high rate of false-positive results (tumor heterogeneity; [9, 10]).

Previous studies have shown that increased levels of free (mobile) lipids are associated with higher grades in brain glioma. Magnetic resonance spectroscopy (MRS) is a noninvasive test approved as a noninvasive modality for assessing lipid concentration and tumor grade [10, 11]. Chemical shift imaging is a gradient-echo (GRE) MRI technique in which in-phase and opposed-phase (IOP) sequences are used clinically to spot lipids in renal angiomyolipoma [12], adrenal adenoma [13], bone marrow involvement [14], and whole-body fat quantification [15]. It could also be useful for detecting lipids in brain gliomas [16]. Elevated levels of HGG lipids may indicate greater loss of signal in the opposed-phase sequences [8, 17, 18]. The advantages of chemical shift IOP sequences are the shorter acquisition time, non-sensitivity to adjacent bone artifacts, wide applicability in MRI devices, general evaluation of the abundance of lipids, and no need

for high-priced software applications and expertise [11, 19].

In the current study, we evaluated the in-phase and opposed-phase sequences for distinguishing HGG from LGG and their correlation with MRS results.

Methods

Participants

This retrospective observational study of prospectively collected preoperative imaging data was approved by the research registrar of Mashhad University of Medical Sciences and was conducted between September 2020 and October 2022 at Ghaem Hospital in Mashhad, Iran. Written consent was obtained from all participants. This study was conducted with patients with brain tumors who were referred to our Brain MRS Center. Inclusion criteria were patient age ≥ 18 years, untreated brain tumor, and MRS images of acceptable quality. The gold standard for diagnosis was based on the World Health Organization (WHO) classification of gliomas [2]. Brain tumors were divided into low-grade (WHO grades 1 and 2) and high-grade (WHO grades 3 and 4) groups [2, 3]. All histopathological examinations were derived from the total or partial resection. Once pathology results were generated, patients with diagnoses other than glioma were excluded from the study. ◘ **Figure** 1 illustrates the selection process.

Imaging and data acquisition

A standard tumor protocol included axial FLAIR (TR, 9000 ms; TE, 114 ms; section thickness, 5 mm), T2-weighted (TR, 4000 ms; TE, 90 ms; section thickness, 5 mm), and T1-weighted (TR, 500 ms; TE, 14 ms; section thickness, 5 mm) images; coronal T1- and T2-weighted images; post-contrast T1-weighted, diffusion weighted imaging (DWI) with derived apparent diffusion coefficient (ADC; TR, 3200 ms; TE, 68 ms; section thickness, 5 mm); and single-voxel spectroscopy (SVS) images (TR, 1500 msec; TE, 35 msec, and a VOI of $1 \times 1 \times 1\,cm3$), which were acquired using a 1.5-T MRI scanner (Ingenia®, Philips
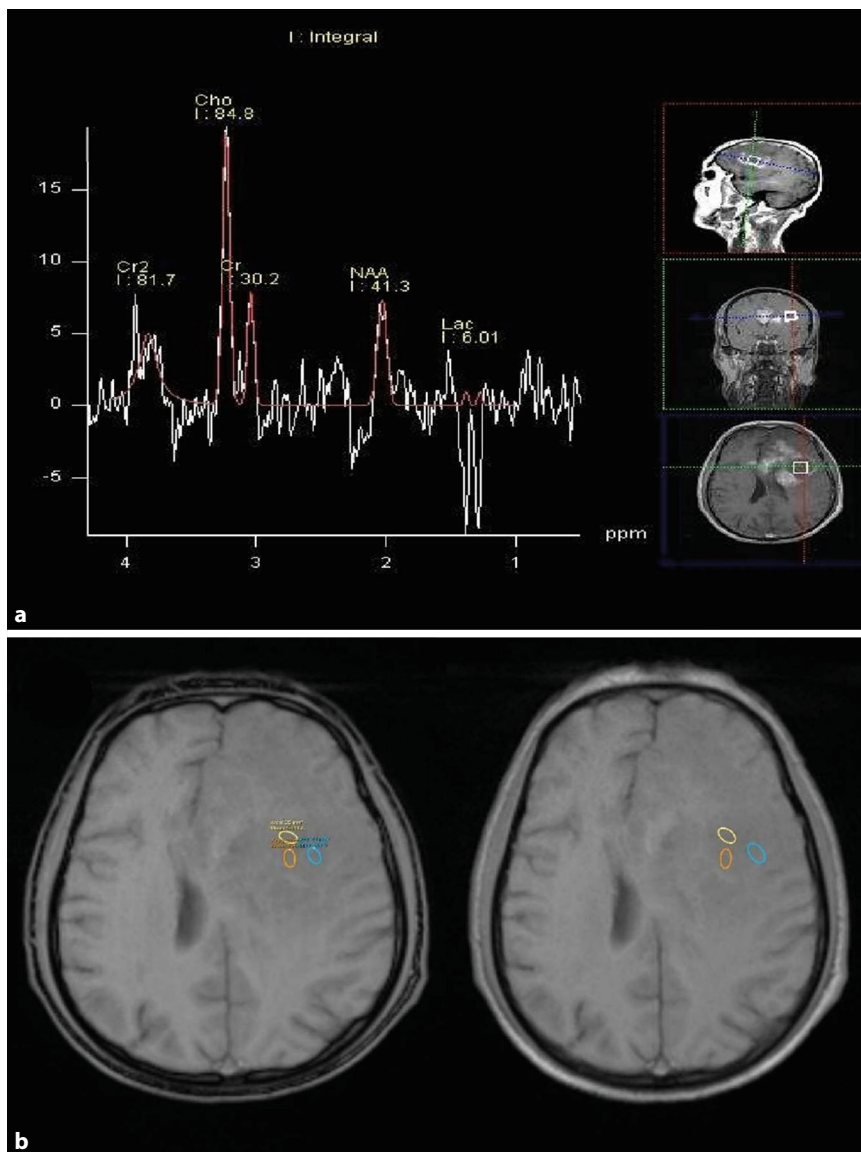
Fig. 2 ▲ A 60-year-old man with high-grade glioma. **a** Magnetic resonance spectroscopy (*MRS*) showed elevated choline and low *N*-acetylaspartate (*NAA*) levels with lactate peak. **b** Three regions of interest were placed on each chemical shift sequence (*right*: opposed-phase, *left*: in-phase) to calculate the mean signal intensities and corresponding signal loss ratio

part of the tumor is defined as the part of the tumor that is isointense on T1-weighted (T1W) images and presents an iso- to hyperintense signal on T2-weighted (T2W) images. The same "solid component" was used on both SVS and IOP imaging analyses. Based on the presence of the decreased SI area in the opposed-phase sequences by visual evaluation, we found the most suitable location for the ROI. The same ROIs were then used consistently across both sequences (**Fig. 2**).

The signal loss ratio (SLR) was calculated using the following formula for estimating intravoxel fat content:

$$SLR_{tumor} = (SI_{In\ phase} - SI_{Opposed\ phase}) / SI_{In\ phase}$$

Both quantitative (concentration: area under the curve) and qualitative (peak presence: yes/no) MRS measurements of lipid-lactate and free lipid were extracted. Demographic information such as age and gender were extracted from the files.

Spectroscopic data quality was systematically evaluated across all examinations. Consistency and reliability were ensured by assessing factors such as noise levels, calibration, and precision.

Data analysis

Based on previous work, a sample size of 20 was estimated (α error: 0.05 and power: 80%) [17]. Numerical variables are expressed as mean ± standard deviation (SD). Qualitative variables are expressed as numbers and percentages. The independent sample *t* test and chi-square test were used to compare parameters between the two groups. The correlation between the average SLR and the concentrations of different lipids was assessed with the Pearson correlation test. Receiver operating characteristic (ROC) curve analysis was performed to find the optimal threshold for the SLR and to assess its diagnostic performance. The diagnostic power of the test was graded as follows: 0.5–0.6, fail; 0.6–0.7, poor; 0.7–0.8, fair; 0.8–0.9, good, 0.9–1, excellent [20]. We used IBM SPSS Statistics for Windows, Version 25.0 (IBM Corp., Armonk, NY, USA) for the data analysis. Statistical significance was set at *p* < 0.05.
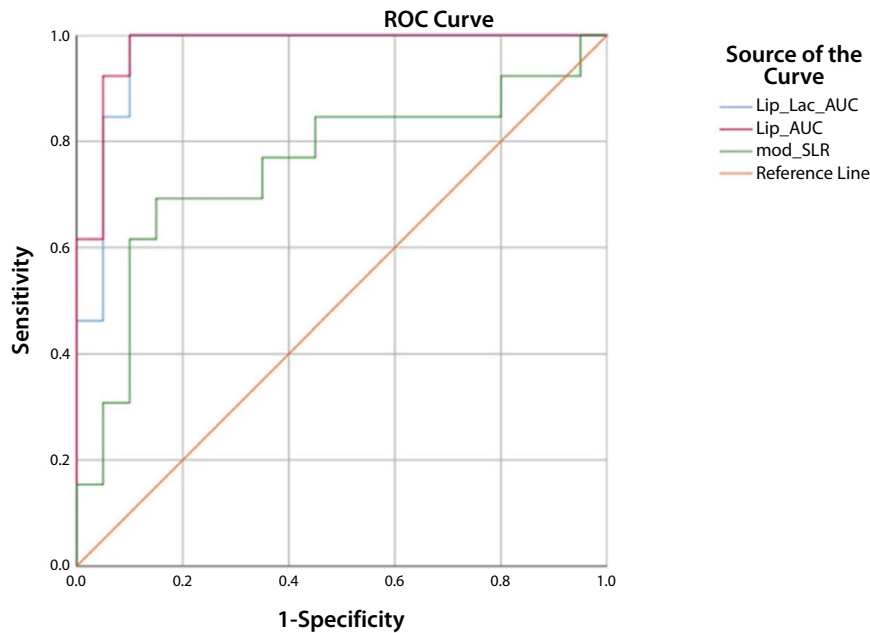
[Amsterdam, the Netherlands]) that was provided with a head coil.

Before administration of the contrast agent, extra chemical shift GRE IOP sequences were acquired. Chemical shift IOP parameters were as follows: repetition time of 160 ms; echo time of 2.4 ms for the in-phase and 4.2 ms for the opposed-phase; flip angle, 80°; section thickness, 5 mm; number of averages = 1; field of view, 250×250 mm^2; matrix size, 256×256. On SVS, free lipid concentration was estimated based on the area under the curve (AUC) at 0.9 and 1.3 ppm peaks. Con-

trast-enhanced series were obtained after intravenous administration of gadoterate meglumine (Dotarem®, Guerbet [Aulnay sous Bois, France]) at a dose of 0.2 mL/kg and a flow rate of 2 mL/s.

An expert radiologist examined the in-phase and opposed-phase images. Three 20–30-mm^2 oval regions of interest (ROIs) were placed manually in the solid component in the in-phase and opposed-phase images, and the average signal intensity (SI) values were determined. The ROI was taken from the same solid area from which the MRS sequence was obtained. The solid

Fig. 3 ▲ Receiver operating characteristic (*ROC*) analysis of lipid lactate concentration, lipid concentration, and signal loss ratio (*SLR*) for distinguishing between low-grade and high-grade gliomas. *AUC* area under the curve

Results

Participants

This study was performed with 33 patients: 20 patients were included in the low-grade and 13 in the high-grade group. The patient ages ranged from 18 to 75 years (43.36 ± 15.192). The study comprised 18 (54.5%) male patients and 15 (45.5%) female patients. The correlation between SLR, age, and gender was not statistically significant ($p = 0.051$ and 0.382, respectively).

Tumor characteristics

In order of frequency, the most common tumor location was frontal lobe (39.4%), temporal lobe (33.3%), parietal lobe (12.1%), pons (9.1%), and thalamus (6.1%).

The mean lipid-lactate concentration in HGG and LGG was 61.41 ± 89.7 and 3.51 ± 7.49, respectively ($p = 0.007$). The mean free lipid concentration in HGG and LGG was 22.13 ± 18.6 and 2.07 ± 2.76, respectively ($p < 0.001$). Both showed statistically significant differences.

A lipid-lactate peak was present in 14 tumors. The mean SLR of present and non-present peaks was 3.73 ± 2.2 and 1.47 ±

1.63, respectively. A comparison of the SLR between the two groups of present and non-present peaks showed a statistically significant difference ($p = 0.004$). A mobile lipid peak was present in 12 tumors. The mean SLR of the present and non-present peaks was 3.64 ± 2.3 and 1.74 ± 1.82, respectively. A comparison of the SLR between the two groups of present and non-present free lipid showed a statistically significant difference ($p = 0.024$).

The mean SLR in the HGG and LGG groups was 3.66 ± 2.12 and 1.63 ± 1.86, respectively. There was a significant difference in the SLR value of the two groups ($p = 0.01$). According to the results of a Pearson test, there was a statistically significant correlation between lipid-lactate (0.48, $p = 0.004$) and free lipid (0.44, $p = 0.009$) concentrations on MRS with SLR. Details of the patient and tumor characteristics and the comparison of the two groups are shown in ◘ **Table** 1.

Diagnostic performance

The ROC analysis of lipid-lactate concentration showed an AUC of 0.96 and an optimal cut-off of 7.74, leading to a sensitivity of 100% and a specificity of 90%. The AUC for lipid concentration was 0.97 and the optimal cut-off was 5.2, leading

to a sensitivity of 100% and a specificity of 90%. The AUC for SLR was 0.75 and the optimal cut-off was 2.88, leading to a sensitivity of 69% and a specificity of 85% (◘ **Table** 2 and ◘ **Fig.** 3).

Discussion

Our results suggest that SLR could be a useful parameter for discriminating between LGG and HGG. Using ROC analysis, we found an optimal threshold (2.88) with which to distinguish between HGG and LGG. It also showed a statistically significant correlation with the presence of free lipids and lipid-lactate peaks in the MRS sequences. We compared the SLR with the estimated concentration of lipid-lactate and lipid in MRS, a well-established method for grading glioma over the past two decades. The results showed a good positive and statistically significant correlation between these two modalities.

Energy production in the brain occurs solely through the glucose mechanism, and the presence of lactate is associated with impaired normal brain mechanisms [21]. In this case, the accumulation of lactate in the brain is due to O_2 deficiency (ischemic changes), increased glycolysis [22], or necrosis [23], which is observed in all tumor grades. Elevated lactate concentrations can be seen in both benign and malignant tumors [23] but the combined lipid-lactate peak is associated with HGG [24]. While lipids are normally found in cell membranes and myelin sheaths, damage and necrosis in high-grade brain tumors cause them to convert to mobile lipids [25]. The distinct lipid peak in MRS is associated with glioblastoma (grade 4; [24]). The presence of these two peaks has been suggested in several studies to differentiate between low-grade and high-grade brain gliomas. In our study, we found a statistically significant difference between SLR in tumors and the presence of these two elements. In contrast to MRS, the IOP can localize the abnormality and receive signals from anatomically defined regions. This is an important difference in the brain because most brain abnormalities are focal and the layer of cranial fat that surrounds the brain contains significant amounts of the same compounds found in the abnormalities.

Table 1 Patient and tumor characteristics

	Low-grade glioma n=20					High-grade glioma n=13					p
	N (%)	Mean±SD	Median	Min	Max	N (%)	Mean±SD	Median	Min	Max	
Age (years)	–	40.45±15.95	40.5	18	75	–	47.85±13.28	54	29	64	–
Female	11 (55%)	–	–	–	–	4 (30.8%)	–	–	–	–	–
Male	9 (50%)	–	–	–	–	9 (50%)	–	–	–	–	–
Lipid-lactate concentration[a]	–	3.51±7.49	1.27	0	32.6	–	61.41±89.7	26	9.86	340.83	0.007*
Lipid-lactate peak	2(10%)	–	–	–	–	12(92.3%)	–	–	–	–	<0.001**
Mobile lipid concentration[a]	–	2.07±2.76	0.96	0	11	–	22.13±18.6	16.66	5.7	70.41	<0.001*
Mobile Lipid peak	1(5%)	–	–	–	–	11(84.6%)	–	–	–	–	<0.001**
Signal loss ratio (SLR)	–	1.63±1.86	1.49	–3.02	5.73	–	3.66±2.12	3.87	–0.05	6.95	0.01*

SD standard deviation, *Min* minimum, *Max* maximum, *N* number
[a]Area under the curve, Magnetic resonance spectroscopy
*Independent *t* test, ** ⁱhi-square test

A study by Norlisah Ramli et al. [8] compared the use of chemical shift IOP sequences in 3-T MRI with MRS for glioma grading. Their study included 22 patients, compared with 33 patients in our study; there were nine cases of LGG (all of them grade 2) and 13 of HGG. They showed a strong correlation between lipid concentration and SLR, and they expressed the SLR as median and interquartile range (IQR) values. Also, they found a significant SLR with advancing a grade. The optimal cut-off for discriminating between the two groups in their study was 0.064 versus 2.88 in our study, but they did not report the sensitivity and specificity of this value. The difference between these values in the study by Norlisah Ramli et al. and our study may be due to different magnetic fields, smaller sample size, and lack of sufficient grade 1 and grade 3 gliomas (only two patients). Pathological confirmation in their investigation derived from biopsies and could be affected by glioma heterogeneity and sampling error.

Another investigation conducted by De Pardieu et al. [18] showed that an SLR of >9% and an SLR of >20% could discriminate between grades 2–3 and grades 3–4, respectively. An AUC equal to 1 demonstrated 100% sensitivity and specificity for differentiating grade 2 and 3 gliomas in their study. Since the therapeutic approach is the same for grade 3 and 4 gliomas, we divided our patients into two groups (LGG and HGG). So far, our results could not be fully compared with their study due to this grouping approach, the SLR estimation formulas, and the use of MRI scanners with different magnetic fields. Furthermore, we also compared the measured fat content (by MRS) with the SLR and found a significant correlation.

Today, 3-T MRI is routinely used for MRS. Our sample size was relatively small and we also did not examine the reproducibility of SLR measurements (interobserver agreement). We attempted to reduce the impact of glioma heterogeneity on our measurements by using three ROIs. These were limitations in our study. We believe that larger multicenter studies are needed to confirm our results. Employing 3D tumor segmentation in future studies for measuring sequences across the entire 3D tumor

Table 2 Diagnostic performance

Parameters	AUC[a] (95% CI)	p	Optimal cut-off[b]	Sensitivity (%)[c]	Specificity (%)[c]	Diagnostic power
Lipid lactate concentration	0.96(0.9–1)	< 0.001	> 7.74	100	90	Excellent
Lipid concentration	0.97(0.93–1)	< 0.001	> 5.2	100	90	Excellent
Signal loss ratio (SLR)	0.75(0.56–0.94)	0.01	> 2.88	69	85	Fair

AUC area under the curve, *CI* confidence interval
[a]ROC analysis
[b]Youden index
[c]Percentages are rounded

volume may offer more reliable statistical calculations with more data points, especially in calculations of in-phase opposed-phase sequences.

Conclusion

The signal loss ratio is a simple, rapid, and noninvasive marker for differentiating between low-grade and high-grade gliomas. There is a significant correlation with both the concentration and presence of free lipid and lipid-lactate peaks in magnetic resonance spectroscopy.

Corresponding address

Afshar Ghamari Khameneh, MD
Department of Radiology, Faculty of Medicine, Imam Reza Hospital, Mashhad University of Medical Sciences
Razi Sq., Mashhad, Iran
Afsharghamari@gmail.com

Declarations

Conflict of interest. B. Abbasi, A.G. Khameneh, H.Z. Soltaniye, G.D.H. Amirkhiz, E. Karimi and R. Akhavan declare that they have no competing interests.

This retrospective observation study of a prospectively collected pre-operative imaging data was approved by the Research Registrar of Mashhad University of Medical Sciences, and was conducted between September 2020 and October 2022 at Ghaem Hospital in Mashhad. Written consent was obtained from all participants.

The supplement containing this article is not sponsored by industry.

References

1. Hess KR, Broglio KR, Bondy ML (2004) Adult glioma incidence trends in the United States, 1977–2000. Cancer 101(10):2293–2299. https://doi.org/10.1002/cncr.20621
2. Louis DN, Perry A, Wesseling P, Brat DJ, Cree IA, Figarella-Branger D et al (2021) The 2021 WHO classification of tumors of the central nervous system: a summary. Neuro Oncol 23(8):1231–1251. https://doi.org/10.1093/neuonc/noab106
3. Wen PY, Packer RJ (2021) The 2021 WHO classification of tumors of the central nervous system: clinical implications. Neuro Oncol 23(8):1215–1217. https://doi.org/10.1093/neuonc/noab120
4. Sanai N, Berger MS (2008) Glioma extent of resection and its impact on patient outcome. Neurosurgery 62(4):753–764. https://doi.org/10.1227/01.neu.0000318159.21731.cf (discussion 264–6)
5. Ostrom QT, Gittleman H, Farah P, Ondracek A, Chen Y, Wolinsky Y et al (2013) CBTRUS statistical report: primary brain and central nervous system tumors diagnosed in the United States in 2006–2010. Neuro Oncol 15(Suppl 2):ii1–56. https://doi.org/10.1093/neuonc/not151
6. Jung KW, Yoo H, Kong HJ, Won YJ, Park S, Lee SH (2012) Population-based survival data for brain tumors in Korea. J Neurooncol 109(2):301–307. https://doi.org/10.1007/s11060-012-0893-5
7. Stewart LA (2002) Chemotherapy in adult high-grade glioma: a systematic review and meta-analysis of individual patient data from 12 randomised trials. Lancet 359(9311):1011–1018. https://doi.org/10.1016/s0140-6736(02)08091-1
8. Ramli N, Khairy AM, Seow P, Tan LK, Wong JH, Ganesan D et al (2016) Novel application of chemical shift gradient echo in- and opposed-phase sequences in 3 T MRI for the detection of H-MRS visible lipids and grading of glioma. Eur Radiol 26(7):2019–2029. https://doi.org/10.1007/s00330-015-4045-0
9. Guzman-De-Villoria JA, Mateos-Perez JM, Fernandez-Garcia P, Castro E, Desco M (2014) Added value of advanced over conventional magnetic resonance imaging in grading gliomas and other primary brain tumors. Cancer Imaging 14:35. https://doi.org/10.1186/s40644-014-0035-8
10. Bulik M, Jancalek R, Vanicek J, Skoch A, Mechl M (2013) Potential of MR spectroscopy for assessment of glioma grading. Clin Neurol Neurosurg 115(2):146–153. https://doi.org/10.1016/j.clineuro.2012.11.002
11. van Werven JR, Hoogduin JM, Nederveen AJ, van Vliet AA, Wajs E, Vandenberk P et al (2009) Reproducibility of 3.0 Tesla magnetic resonance spectroscopy for measuring hepatic fat content. J Magn Reson Imaging 30(2):444–448
12. Israel GM, Hindman N, Hecht E, Krinsky G (2005) The use of opposed-phase chemical shift MRI in the diagnosis of renal angiomyolipomas. AJR Am J Roentgenol 184(6):1868–1872. https://doi.org/10.2214/ajr.184.6.01841868
13. Namimoto T, Yamashita Y, Mitsuzaki K, Nakayama Y, Makita O, Kadota M et al (2001) Adrenal masses: quantification of fat content with double-echo chemical shift in-phase and opposed-phase FLASH MR images for differentiation of adrenal adenomas. Radiology 218(3):642–646. https://doi.org/10.1148/radiology.218.3.r01mr15642
14. Seiderer M, Staebler A, Wagner H (1999) MRI of bone marrow: opposed-phase gradient-echo sequences with long repetition time. Eur Radiol 9(4):652–661. https://doi.org/10.1007/s003300050727
15. Outwater EK, Blasbalg R, Siegelman ES, Vala M (1998) Detection of lipid in abdominal tissues with opposed-phase gradient-echo images at 1.5 T: techniques and diagnostic importance. Radiographics 18(6):1465–1480. https://doi.org/10.1148/radiographics.18.6.9821195
16. Lim C, Ng K, Ramli N, Azman RJR (2011) Evaluation of the application of chemical shift for the detection of lipid in brain lesion. Radiography 17(1):43–48
17. Seow P, Narayanan V, Hernowo AT, Wong JHD, Ramli N (2018) Quantification and visualization of lipid landscape in glioma using in -and opposed-phase imaging. neuroimage Clin 20:531–536. https://doi.org/10.1016/j.nicl.2018.08.003
18. De Pardieu M, Boucebci S, Herpe G, Fauche C, Velasco S, Ingrand P et al (2020) Glioma-grade diagnosis using in-phase and out-of-phase T1-weighted magnetic resonance imaging: a prospective study. Diagn Interv Imaging 101(7–8):451–456. https://doi.org/10.1016/j.diii.2020.04.013
19. Ragab Y, Emad Y, Gheita T, Mansour M, Abou-Zeid A, Ferrari S et al (2009) Differentiation of osteoporotic and neoplastic vertebral fractures by chemical shift {in-phase and out-of phase} MR imaging. Eur J Radiol 72(1):125–133. https://doi.org/10.1016/j.ejrad.2008.06.019
20. Nahm FS (2022) Receiver operating characteristic curve: overview and practical use for clinicians. Korean J Anesthesiol 75(1):25–36. https://doi.org/10.4097/kja.21209
21. McKnight TR (2004) Proton magnetic resonance spectroscopic evaluation of brain tumor metabolism. Semin Oncol 31(5):605–617
22. Tien RD, Lai PH, Smith JS, Lazeyras F (1996) Single-voxel proton brain spectroscopy exam (PROBE/SV) in patients with primary brain tumors. AJR Am J Roentgenol 167(1):201–209. https://doi.org/10.2214/ajr.167.1.8659372

23. Fulham MJ, Bizzi A, Dietz MJ, Shih HH, Raman R, Sobering GS et al (1992) Mapping of brain tumor metabolites with proton MR spectroscopic imaging: clinical relevance. Radiology 185(3):675–686. https://doi.org/10.1148/radiology.185.3.1438744

24. Nakamura H, Doi M, Suzuki T, Yoshida Y, Hoshikawa M, Uchida M et al (2018) The significance of lactate and lipid peaks for predicting primary neuroepithelial tumor grade with proton MR spectroscopy. Magn Reson Med Sci 17(3):238–243. https://doi.org/10.2463/mrms.mp.2017-0042

25. Sijens PE, Levendag PC, Vecht CJ, van Dijk P, Oudkerk M (1996) 1H MR spectroscopy detection of lipids and lactate in metastatic brain tumors. NMR Biomed 9(2):65–71. https://doi.org/10.1002/(sici)1099-1492(199604)9:2⟨65::Aid-nbm397⟩3.0.Co;2-n

Zusammenfassung

Anwendung der Bildgebung mittels chemischer Verschiebung (gleichphasig/gegenphasig) zur Differenzierung zwischen niedriggradigen und hochgradigen Gliomen und Vergleich mit der Magnetresonanzspektroskopie

Hintergrund: Die Einstufung von Gliomen ist für Therapieentscheidungen und die Patientenprognose essenziell. In der vorliegenden Studie wurden gleichphasige und phasenverschobene Sequenzen zur Unterscheidung hochgradiger (HGG) von niedriggradigen Gliomen (LGG) sowie die Korrelation mit den Ergebnissen der Magnetresonanzspektroskopie (MRS) untersucht.

Methoden: Die vorliegende Beobachtungsstudie umfasste Patienten mit Hirntumoren, die an die Klinik der Autoren zur Hirn-MRS überwiesen worden waren. Der Goldstandard für die Diagnose basierte auf der Klassifikation der Gliome seitens der Weltgesundheitsorganisation (WHO). Es wurde ein Standardtumorprotokoll unter Einsatz eines 1,5-T-MRS-Geräts durchgeführt. Vor Applikation des Kontrastmittels wurden zusätzliche gleichphasige und phasenverschobenen Sequenzen akquiriert. In die solide Komponente wurde 3 ovale Bereich von Interesse („regions of interest", ROI) mit einer Größe von 20–30-mm^2 gesetzt, und das Signal-Verlust-Verhältnis („signal loss ratio", SLR) wurde mittels der folgenden Formel berechnet:

$$SLR_{Tumor} = (SI_{Gleichphasig} - SI_{Gegenphasig}) / SI_{Gleichphasig}$$

Korrelationen und Vergleiche zwischen den Gruppen wurden unter Verwendung des Pearson-Tests, des Chi-Quadrat-Tests und des t-Tests für unabhängige Stichproben durchgeführt. Um die diagnostische Leistungsfähigkeit zu ermitteln, erfolgte eine Receiver-Operating-Characteristic(ROC)-Kurvenanalyse. Die statistische Signifikanz wurde bei $p < 0,05$ festgesetzt.

Ergebnisse: In die LGG-Gruppe wurden 20 und in die HGG-Gruppe 13 Patienten eingeteilt. Der mittlere SLR in der HGG- und LGG-Gruppe betrug $3,66 \pm 2,12$ bzw. $1,63 \pm 1,86$ ($p = 0,01$). Eine statistische signifikante Korrelation bestand zwischen den Konzentrationen von Lipidlaktat (0,48; $p = 0,004$) sowie freiem Lipid (0,44; $p = 0,009$) in der MRS und dem SLR.

Schlussfolgerung: Der SLR ist ein einfacher, schneller und nichtinvasiver Marker zur Unterscheidung zwischen LGG und HGG. Es gibt eine signifikante Korrelation sowohl mit der Konzentration als auch mit dem Vorliegen von Peaks von freiem Lipid und Lipidlaktat in der MRS.

Schlüsselwörter

MRI · Cerebral · Magnetresonanzspektroskopie · Gliom · Hirntumor